



pH-sensitive chitosan-PEG-decorated hollow mesoporous silica nanoparticles could be an effective treatment for acute myeloid leukemia (AML)

G. Ultav · H. Tonbul · E. Tavukcuoglu · S. C. Ozturk · S. Akbas · A. Sahin · G. Esendagli · Y. Capan

Received: 6 June 2021 / Accepted: 6 January 2022 / Published online: 10 February 2022
© The Author(s), under exclusive licence to Springer Nature B.V. 2022

Abstract Improved treatment of acute myeloid leukemia (AML) could be possible by longer retention of anticancer drugs in the bloodstream. In this study, it was aimed to obtain improved treatment against AML by providing prolonged blood levels of doxorubicin and ensuring endosomal escape by the proton sponge effect. With this aim, pH-sensitive and chitosan-poly ethylene glycol (Cs-PEG) coated doxorubicin-loaded hollow mesoporous silica nanoparticles (C-HMSN-DN) were prepared. Nanoparticles (NPs) were characterized by dynamic light scattering (DLS), zeta potential, transmission electron microscopy (TEM), X-Ray diffraction (XRD), and nitrogen adsorption-desorption isotherms. High doxorubicin encapsulation efficacy was obtained as 90%. pH-sensitive formulations were showed higher cellular uptake and

found more effective against human leukemia cell line (HL60) than non-pH sensitive formulations. In vivo studies showed that Cs-PEG coating prolonged blood circulation time tremendously in comparison to unmodified nanoparticles and free doxorubicin. The designed drug delivery system (DDS) can be more effective by endosomal escape to eliminate myeloid cells which are granular cells containing a great number of lysosomes. In conclusion, we present a drug delivery system that provides a prolonged blood circulation time due to Cs-PEG coating and effective drug delivery via pH-sensitive drug release and endosomal escape for AML treatment.

Keywords Drug delivery · Hollow mesoporous silica nanoparticles (HMSN) · Chitosan-PEG · Doxorubicin · Acute myeloid leukemia (AML)

Supplementary Information The online version contains supplementary material available at <https://doi.org/10.1007/s11051-022-05404-8>.

G. Ultav
Department of Nanotechnology and Nanomedicine, Grad School of Science and Engineering, Hacettepe University, Ankara, Turkey
e-mail: gozdeultav@gmail.com

H. Tonbul
Department of Pharmaceutical Technology, Faculty of Pharmacy, Inonu University, Malatya, Turkey

E. Tavukcuoglu · G. Esendagli
Department of Basic Oncology, Hacettepe University Cancer Institute, Ankara, Turkey

S. C. Ozturk
Laboratory Animals Research And Application Centre (HUDHAM), Hacettepe University, Ankara, Turkey

S. Akbas · Y. Capan (✉)
Department of Pharmaceutical Technology, Faculty of Pharmacy, Hacettepe University, Ankara, Turkey
e-mail: ycapan@hacettepe.edu.tr

A. Sahin
Department of Pharmacy Service, Vocational School of Health Services, Bilecik Seyh Edebali University, Bilecik, Turkey

Introduction

Acute myeloid leukemia (AML) is a type of cancer that begins in the bone marrow (Robbins and Kumar 2008). Although the survival rate has increased in recent years, AML can still be fatal to many patients (Stewart and Wild 2014). Chemotherapy is one of the strategies for the treatment, and doxorubicin (Dox) is one of the most used anthracyclines in the clinic. Repeated doses are required in the clinic since Dox eliminates blood in minutes which is inconvenient for patient compliance (Krischke et al. 2016). Doxorubicin inhibits nucleic acid synthesis at a cancer cell by intercalation with DNA like other anthracyclines (Yoo et al. 2016). It can be used for the treatment of primary ovarian cancer, lung, thyroid, breast cancers, and some kinds of sarcomas and leukemia. However, it is highly toxic and eliminates from blood in minutes resulting inefficient therapy. Doxil is the nano-technological formulation of doxorubicin that overcomes some of these problems; still more progress can be achieved by developing nanoparticles (NPs) as stimuli-responsive carriers which can be triggered by pH, enzyme, or temperature (Kanwal et al. 2018). The main advantages of these systems are reducing repeated doses and increasing patient compliance.

Hollow mesoporous silica nanoparticles (HMSNs) are highly impressive due to their high internal volume and highly permeable mesoporous shell (Fang et al. 2013). HMSNs are good candidates for drug delivery due to their high internal volume, adjustable porosity, easy modification of the surface, etc. (García-Fernández et al. 2020; Llopis-Lorente et al. 2017). Templating methods are one of the most effective and common methods used in HMSN preparation (Fang et al. 2013).

One of the useful approaches for avoiding non-targeted toxicity is exploiting the difference between the normal cells and cancer cells like lower pH levels, high amount of glutathione, or overexpressed molecules on membrane such as folic acid. Drug delivery systems (DDSs) can be designed to provide triggered release in an acidic environment exploiting the pH of the cytosol around 5–5.5. A pH-sensitive system provides prevention of drug release in normal physiological conditions which are close to neutral pH until they reach cancer cells which are more acidic. By this means, the reduced drug-healthy tissue/cell

interaction elicits minimized side effects (Torchilin 2018; Rawal 2018; Wang et al. 2018).

NPs are taken into the cell by various pathways depending on the particle size and/or shape (Herd et al. 2013). However, the endocytic pathway can be defined as the basic cellular uptake mechanism for NPs (Roca and Haes 2008). When a NP interacts with the cell membrane, the membrane collapses and creates a vesicle containing NP which is called an endosome vesicle with a pH of 5–6. This early endosome travels to the late endosome to conclude a fusion with the lysosome which contains digestive enzymes (Roca and Haes 2008). Therefore, nanoparticles are digested in the lysosome; the bioavailability of cargo drugs decreases.

At this point, by utilizing the low pH of the endosome, the bioavailability can be increased by designing particles that release only at lower pH (Ke et al. 2011). In addition, systems have been designed to overcome the endosomal entrapment before reaching the lysosome and to deliver the drug substance released at low pH to the cytosol (Varkouhi et al. 2011). There are some mechanisms with different routes for endosomal escape: pore formation in the endosome vesicle, pH-buffer effect (proton sponge effect), and photochemical disruption of the endosome vesicle (Ke et al. 2011). The most important and the most widely researched of these mechanisms is the proton sponge effect where a weak base released from NPs reacts with acidic media in the endosome and produces CO₂ gas that creates pressure inside of the vesicle to erupt which will lead to a better distribution of the drug in the cell (Varkouhi et al. 2011).

Elimination of NPs from blood instantly is another issue. The enhanced permeability and retention (EPR) effect is the property characterized by increased accumulation of NPs in tumor tissues due to leaky vasculature and reduced lymphatic drainage as a result of pathologic conditions. EPR-mediated tumor accumulation is a result of long-circulation nanoparticles. However, blank nanoparticles are easily detected by the body and removed from blood (Suk et al. 2016). When the nanoparticle (NP) surface is covered with polyethylene glycol (PEG), the NPs were not recognized by the immune system as a result of a condition called the “stealth effect.” NP surfaces interact with serum proteins called opsonin, which elicits accumulation of NPs in the reticuloendothelial system (RES) system, and this is called opsonization; however, studies show

that PEGylation can reduce the opsonization and hamper the rapid elimination of nanoparticles from blood circulation (Pisani et al. 2017; Behzadi et al. 2017; Gunawan et al. 2014; Fleischer and Payne 2014).

In this study, HMSNs were selected as a drug delivery platform for cancer treatment. It was decided to use the self-templating method due to obtain particles with suitable size and distribution. Doxorubicin, an anticancer agent that can be used in the treatment of AML, has been selected as the drug to obtain a pH-sensitive DDS due to hydrogen bonding between silica and Dox (Inocêncio et al. 2021) exploiting the more acidic nature of the cancer cells. Sodium bicarbonate was co-loaded into the DDS besides the drug substance to ensure endosomal escape by the proton sponge effect. A chitosan-poly ethylene glycol (Cs-PEG) coating on NPs was achieved to obtain a longer blood circulation time. Finally, obtained DDS was fully characterized, and therapeutic efficiency was evaluated by *in vitro* and *in vivo* studies.

Experimental

Materials

All chemicals were purchased from Sigma-Aldrich except doxorubicin hydrochloride which was a kind gift from DEVA Holding A.S. and Cs-PEG was a kind gift from Prof. Fernandez-Megia. The HL60 cell line was supplied by Hacettepe University Basic Oncology Subdivision. Devices for characterization such as transmission electron microscopy (TEM), scanning electron microscopy (SEM), surface characterization (BET), and X-ray diffraction were provided by Middle East Technical University (METU) Central Laboratory.

Preparation of NPs

The self-templating strategy was used to obtain hollow NPs (Fang et al. 2011). First of all, silica NPs were prepared by the Stöber method with minor modifications (Fang et al. 2013, 2011). Briefly, 1.75 mL NH_4OH and 45 mL ethanol were mixed for 15 min, and 2.6 mL water and 0.8 mL tetraethyl orthosilicate

(TEOS) were added to it with constant stirring at 300 rpm. After 1 h, the solution was centrifuged (13,500 rpm, 30 min), washed, and stocked in ethanol (5 mg/mL). Preparation of the porous shell was done using the method indicated by Fang et al. with minor modifications (Fang et al. 2011). Sixty milligrams of these NPs were dispersed in 10 mL water and added to 30 mL of water/ethanol mixture (15:15 v/v) to prepare HMSNs. A 75 mg cetyltrimethylammonium bromide CTAB and 0.274 mL NH_4OH were introduced to the solution. After mixing for 30 min, 0.125 mL of TEOS was added to react and stirred for 6 h at room temperature, at 300 rpm. Then the mixture was centrifuged (13,500 rpm, 30 min), the supernatant was discarded, and NPs were dispersed in 10 mL water by an ultrasonic probe (20%, 15 min). A 220 mg of Na_2CO_3 was dissolved in solution to achieve chemical etching of template silica and stirred at 50 °C overnight. NPs were washed and added to 1% hydrochloric acid solution in ethanol for template removal; NPs were washed and re-dispersed in ethanol for storage.

To obtain fluorescein-5-isothiocyanate (FITC) labeled HMSN; 10 μL of 3-Triethoxysilylpropylamine (APTES) was added to the 100 mg NPs for amine functionalization to achieve FITC labeling followed by overnight mixing. On the other hand, 10 mg FITC was dissolved in methanol, and 5 mg N-Hydroxysuccinimide (NHS), and 5 mg N-(3-Dimethylaminopropyl)-N'-ethyl carbodiimide hydrochloride (EDC) were added to the mixture under continuous stirring. These two solutions were mixed to obtain fluorescent-labeled HMSPs.

Drug loading and Cs-PEG coating

A 0.5 mg/mL doxorubicin solution was prepared in 1 mg/mL NP suspension in PBS and stirred at dark for 12 h. NaHCO_3 was added to the suspension and mixed for another 12 h. After that, Cs-PEG was introduced to the mixture and stirred for 3 h. Final concentration of NaHCO_3 was 0.5 mg/mL and Cs-PEG was 1 mg/mL.

NPs were centrifuged at 20,000g for 30 min and the supernatant was collected and the quantification was done by HPLC. Drug loading efficiency was calculated according to Eq. 1.

$$\text{Drug loading efficiency (\%)} = \frac{\text{total doxorubicin amount (mg)} - \text{doxorubicin in supernatant (mg)}}{\text{total doxorubicin amount (mg)}} \times 100 \quad (1)$$

NP characterization

The particle size and zeta potential of the nanoparticles were measured with Malvern Nano-ZS (Malvern Instruments) at room temperature. Samples were dispersed in distilled water (1:400 dilution), and measurements were given for 3 individual replicates with 173° light scattering angle at 25°C. The morphology of nanoparticles was examined with scanning electron microscopy (SEM) and transmission electron microscopy (TEM) images. For TEM, nanoparticles were dispersed in ethyl alcohol and dropped onto the grid, after drying, analyzed with HR-TEM (Jem Jeol 2100F). Similar preparation steps were applied for field emission SEM (Quanta 400F Field Emission). XRD analysis was conducted to analyze the crystalline structure of nanoparticles and obtained on Rigaku Ultima-IV diffractometer using Cu-K α radiation over the range of 1–10° with a step width of 0.02°. FTIR spectra were conducted to analyze CTAB removal, and Bruker Alpha FTIR spectrometer was used with 4 cm⁻¹ resolution in 4000–400 cm⁻¹ wavenumber region. Nitrogen adsorption-desorption analysis was run for the determination of surface area. Dried samples were degassed at 250°C for 3 h and then analysis was performed by AUTOSORB 6b. All SEM, TEM, XRD, and surface characterization analyses were performed at METU Central Labs.

Drug release study and HPLC conditions

A drug release study was performed in PBS with different pHs at 37 °C shaker for 24 h. The results were calculated cumulatively.

A standard C 18 (250 m×4.6 mm, 5 μ m) column was used under isocratic conditions with a 1-mL/min flow rate at 35 °C. Analyses were performed at 475-nm excitation with a fluorescence detector. The mobile phase was acetonitrile:water (38:62) (Daeihamed et al. 2015).

Cell culture

The HL60 cell line was obtained from American Type Culture Collection (ATCC). Cells were cultured

in RPMI 1640 which was supplemented with 10% fetal bovine serum (FBS), 1% U/mL penicillin, and 1% U/mL streptomycin and incubated in a 5% CO₂ humidified atmosphere at 37 °C.

Cytotoxicity analysis

2,5-diphenyl-2H-tetrazolium bromide (MTT) assay was used to evaluate the cytotoxicity of formulations. 5×10⁴ cells were seeded to 96-well plates in 50- μ L media and incubated for 6 h and then 50 μ L of formulations in media with different concentrations were added. At the end of the incubation periods, 5mg/mL MTT solution (25 μ L) was added to wells and incubated for 4 h. Later, 100 μ L sodium dodecyl sulfate (SDS)/dimethylformamide (DMF)/water (45:55 DMF:water containing 200g SDS) mixture was added to wells to dissolve cells and formazan crystals. After overnight incubation, optical density (OD) was measured at 570 nm with a microplate reader (SpectraMax Plus, Molecular Devices).

Cellular uptake analysis

Cellular uptake of formulations was evaluated by a flow cytometer. 5×10⁵ cells were seeded per well at a 24-well plate and incubated overnight. Three different concentrations of NPs were used. After the incubation of formulations, (containing the same amount of doxorubicin in each group) for 24 h, cells were collected, and the median fluorescence intensity (MFI) of these cells was measured by flow cytometry.

Fluorescence microscopy studies were also performed to show the cellular uptake of HMSNs. 8×10⁵ cells seeded per well at 12-well plate and incubated overnight. Similar to flow cytometer studies, formulations were applied to cells and incubated for 24 h. Then the cells were washed and harvested; cytospin preparations (Universal 320, Hettich, Tuttlingen, Germany) were obtained and fixed with 4% *p*-formaldehyde. Cells were counterstained with DAPI and examined with fluorescence microscopy (Olympus America Inc.). Finally, images were processed using ImageJ software (NIH Image, USA).

Animal study

The animal study was performed to show that whether the PEGylation provides prolonged blood circulation time. Eighteen rats (Sprague Dawley, around 400 g each) were separated into 3 groups ($n=6$) and 3 rats were used as the control group. Groups were organized as below:

- Group 1: Control, Dox in PBS was injected from tail vein (200 μ L saline, 6 mg Dox/kg)
- Group 2: HMSN-DN in PBS was injected from tail vein (200 μ L saline, 6 mg Dox, and mg NaHCO_3 /kg)
- Group 3: C-HMSN-DN in PBS was injected from tail vein (200 μ L saline, 6 mg Dox, and mg NaHCO_3 /kg)

All injections were introduced i.v. as one dose, and after that, 0.5 mL blood was collected 5 times (5 min, 30 min, 2 h, 8 h, and 24 h) from each rat. After the plasma was separated by centrifuge, the samples were analyzed by HPLC after sample preparation steps. This study was performed with the permission of the Hacettepe University Commission of Ethics (2018/63-04).

Doxorubicin quantification from blood

Ammonium acetate buffer (pH=3, 10 mM) and acetonitrile (70:30 v:v) were selected as mobile phases, and C 18 (250 m \times 4.6 mm, 5 μ m) column was the stationary phase. Analyses were performed by fluorescence detector (480 nm excitation and 560 nm emission) with 0.75 mL/min flow rate at 40 $^{\circ}$ C (Chen et al. 2013).

A 2 mL chloroform:methanol solution (4:1 v:v) and 2.5 μ g/mL daunorubicin in 20 μ L methanol as an internal standard were added to a 100 μ L plasma. After vortex for 2 min, samples were centrifuged at 6000 rpm for 10 min. The organic phase was collected and dried under N_2 . The precipitate was dissolved in 100 μ L methanol and centrifuged for another 5 min at 5000 rpm. The supernatant was collected and used for HPLC analyses (50 μ L was the injection volume) (Feng et al. 2014).

Statistics

All the results were given as mean values. Analysis of variance (ANOVA) test was performed for more than two group comparisons by SPSS. The difference between the two groups was regarded as statistically significant when the p value was <0.05 (*).

Results and discussion

Preparation and characterization of NPs

Template silica nanoparticles were synthesized and characterized by Zetasizer and SEM to obtain DDS by the self-templating method (Fig. S1). Monodispersed silica NPs were obtained around 90 nm in size with spherical morphology according to DLS (PI 0.063) and SEM results (Figs. S1 A and 1A), and the zeta potential was about -53 mV shown in Fig. S1 B. These NPs were used as templates for HMSNs, and mesoporous silica NPs were synthesized around them followed by an etching step to obtain a hollow interior.

The size of the obtained HMSNs was about 300 nm by DLS, and the zeta potential was about -30 mV (Fig. S2). After the chitosan-PEG coating, the zeta potential was changed to $+30$ mV which suggests the Cs-PEG was coated on the surface and changed the surface charge (Fig. S3). SEM and TEM revealed that the particles were monodispersed and spherical, and particle size was about 150 nm according to Fig 1B, C, and D. This difference can be explained by the NP-dispersion media interactions affecting the hydrodynamic diameter due to surface hydrophilic silanol groups (Bagwe et al. 2006; Tuoriniemi et al. 2014). Kaasalainen et al. showed that there is a significant difference between particle size measurements by TEM or DLS for silica/mesoporous silica nanoparticles (Kaasalainen et al. 2017). The color contrast between the core and shell indicates the particles have a hollow interior (Fig. S4). Further characterization was performed by FTIR, XRD, and BET to show the surfactant removal, crystalline structure, and surface area and volume, respectively. The results were given in Fig. 2.

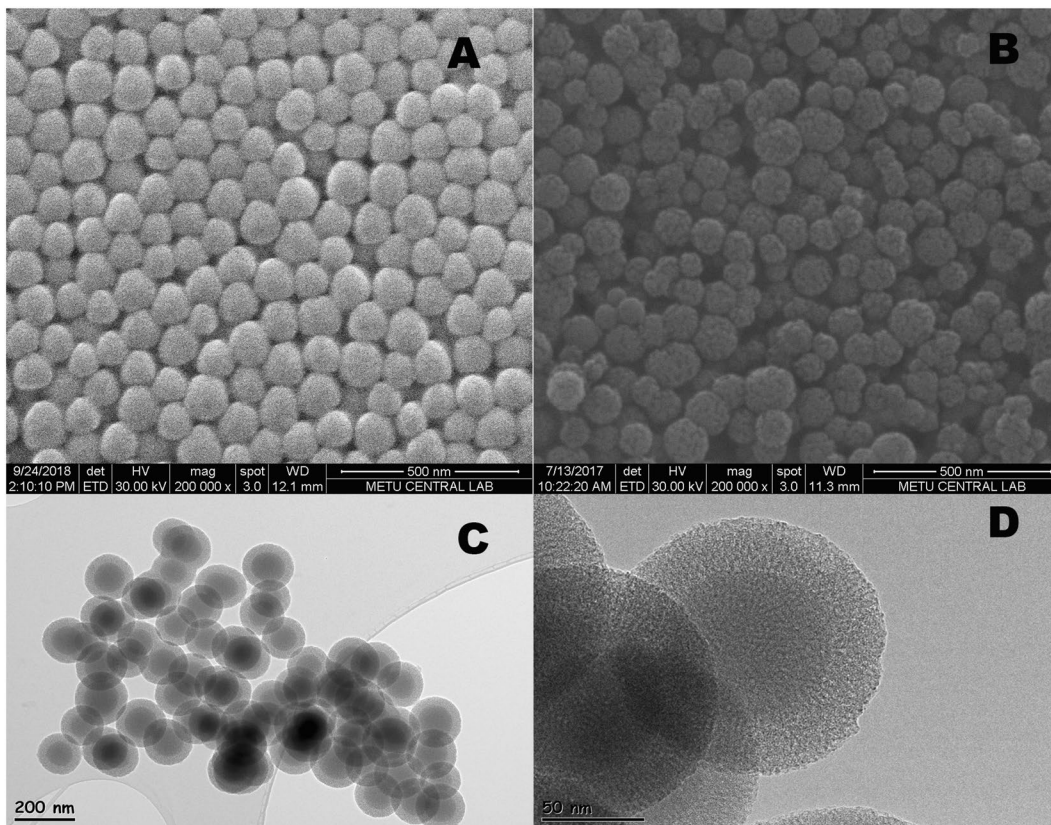


Fig. 1 SEM image of silica NPs and C-HMSN shown in **A** and **B** respectively. TEM images of HMSNs were given in **C** and **D**

After the HMSNs were synthesized and CTAB was removed by acidic ethanol treatment, FTIR was performed to show that the CTAB was removed. The peak at 1080 cm^{-1} indicates the silanol groups on silica NPs. No peak was observed after the extraction with acidic ethanol between 2500 and 3000 cm^{-1} where CTAB peak would be observed due to C-H vibrations of CH_2 groups of CTAB, in Fig 2A. Small-angle XRD results were performed for both Cs-PEG coated and uncoated HMSNs. The peak between 2 and 4° (2θ) shows the typical peak of mesoporous silica presented in Fig 2B which is in compliance with typical MCM-41 peaks (Fang et al. 2011; Chen et al. 2010; Teng et al. 2013). This peak was almost disappeared in Fig. 3C after Cs-PEG coating on the surface. A decrease in 2 – 4° peak of mesoporous silica nanoparticles after chitosan coating was shown in literature before (Daryasari et al. 2016; Szegedi et al. 2012; Popat et al. 2012).

This drop can be explained by chitosan covering the surface. After the CTAB removal by extraction, porosity, inner volume, and pore size were investigated by N_2 adsorption-desorption measurements (Braun-Emmet-Teller method). Type IV isotherm was observed which is typical for mesoporous silica (Zhu et al. 2011). The results were calculated as 216.9 cm^2 for surface area, 0.16 cc/g for volume, and 1.9 nm for pore size respectively; also these results are in compliance with the literature (Chen et al. 2010; Xiong et al. 2015). Pore size distribution was analyzed by Barrett–Joyner–Halend (BJH) which was shown in Fig. 2E, and a narrow pore size distribution was observed with a sharp peak at 3.7 nm .

Drug release studies

Doxorubicin was loaded into HMSNs with or without sodium bicarbonate and then the HMSNs were coated

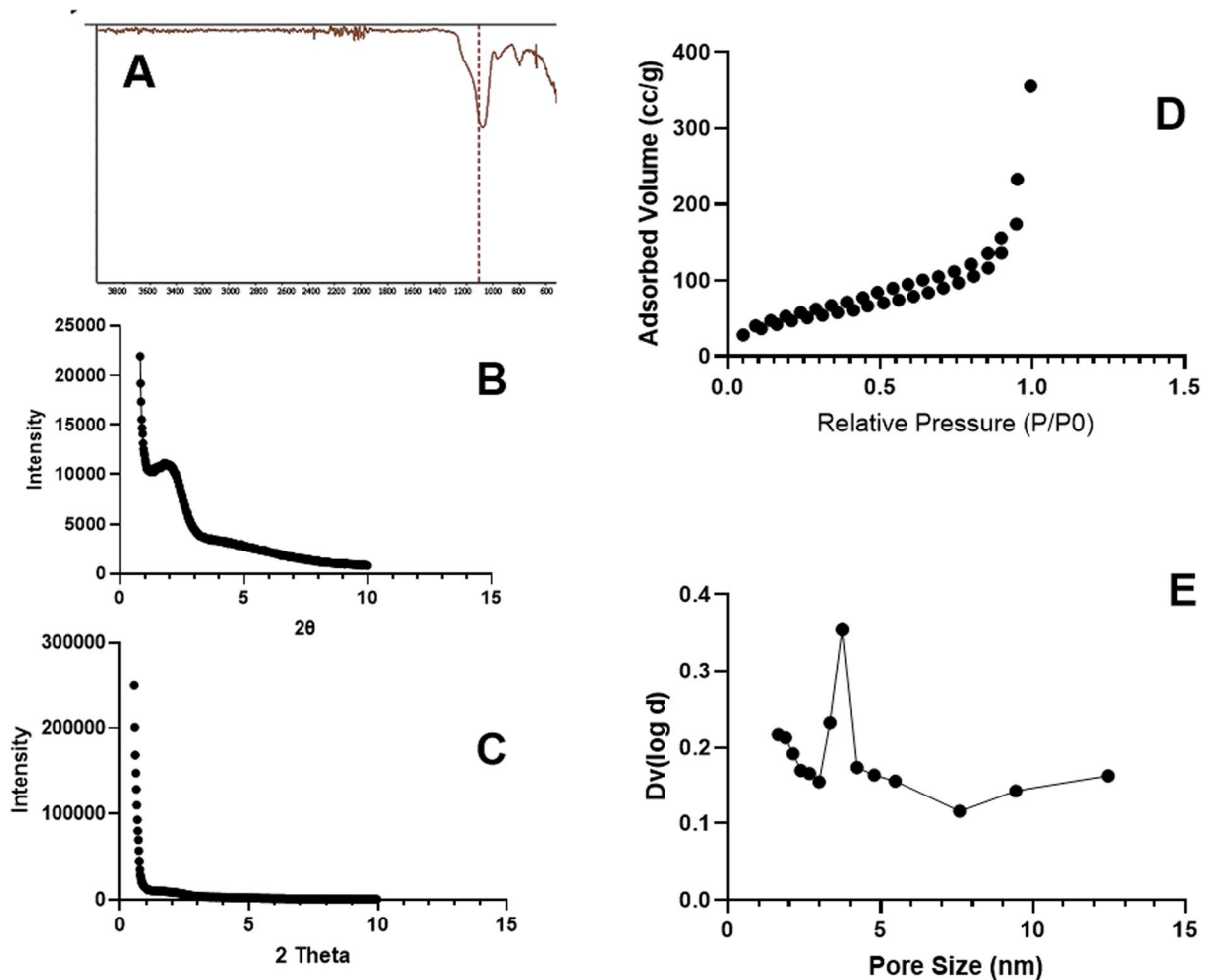


Fig. 2 A FTIR result of hollow mesoporous silica nanoparticles after CTAB template removal. B and C represent XRD graphics of hollow mesoporous silica nanoparticles (HMSN)

and after chitosan coating (C-HMSN) respectively. D and E represent BET results, isotherm, and pore size which were presented, respectively

with Cs-PEG. A formulation was left uncoated to evaluate the effect of coating on drug release and also cellular uptake and cytotoxicity. Drug substance (doxorubicin with or without sodium bicarbonate) was dissolved in PBS and then the NPs were added to the solution and mixed overnight. Then the coating was performed for related formulations by the addition of Cs-PEG to the mixture with at least 6 h under stirring. After that, the NPs were separated from the solution, and the supernatant was analyzed by the HPLC to measure the doxorubicin content. The loaded drug substance was calculated by subtraction of the measured from the added amount to the solution in the first place. The result showed that HMSNs have a high drug loading capacity over 90%, and similar

efficiencies are observed between the formulations. Zhu et al. showed Dox loading efficiency of HMSNs was about 84%, yet the PEGylated HMSNs have an efficiency around 70%, and according to their study, PEGylation has lowered the drug loading efficiency (Zhu et al. 2011). In this study, PEGylation did not affect the drug loading efficiency due to performing after the drug loading. Also according to their study, the drug loading was about 40 µg to 1 mg of NPs (Zhu et al. 2011). This performance was improved in this study to about 0.47 µg Dox to 1 µg HMSN, and the findings were given in Table 1.

Drug release studies at different pHs were important for this study to show pH-triggered release. The hydrogen bonding between Dox and silica surface

Table 1 Drug loading efficiency and drug loading % of formulations

Formulation	Drug loading efficiency (%)	Drug loading % ($\mu\text{g Dox}/\mu\text{g NPs}$)
Doxorubicin-loaded HMSN (HMSN-D)	93.7 ± 5.1	47 ± 2.6
Doxorubicin and NaHCO_3 -loaded HMSN (HMSN-DN)	93.4 ± 2.9	47 ± 1.5
Doxorubicin-loaded and Cs-PEG-coated HMSN (C-HMSN-D)	93.2 ± 4.1	47 ± 2.1
Doxorubicin- and NaHCO_3 -loaded Cs-PEG-coated HMSN (C-HMSN-DN)	96.6 ± 2.1	52 ± 1.1

is sensitive to pH changes which provide the instant drug release in lower pH. By this approach, reducing side effects of drug and delivery of the cargo inside the cancer cell can be achieved due to endosome vesicle has lower pH approximately 5 to 6. To show this, drug release studies were performed at pH 5, pH 6, and pH 7.4 in PBS at 37°C . Drug release was determined for 4 different formulations as Dox-loaded HMSNs (HMSN-D), Dox, and sodium bicarbonate-loaded HMSNs (HMSN-DN) to understand the effect of co-loading on release; Dox-loaded Cs-PEG coated HMSN (C-HMSN-D) to understand the effect of extra coating by polymer and the last formulation as

NaHCO_3 and Dox loaded and Cs-PEG-coated HMSN (C-HMSN-DN). The results are given in Fig. 3, and it can be seen that the Dox release is increasing when the pH is lowering which means the pH-triggered release was achieved.

The minimum drug release of each formulation was observed at pH 7.4 in Fig. 3A, B, C, and D. The higher drug release was achieved at lower pH for every formulation. Figure 3 A and C suggest that NaHCO_3 co-loading increases the drug release in comparison with Fig. 3B and D at each pH due to the presence of Na^+ ions in the media. No significant difference of drug release was observed

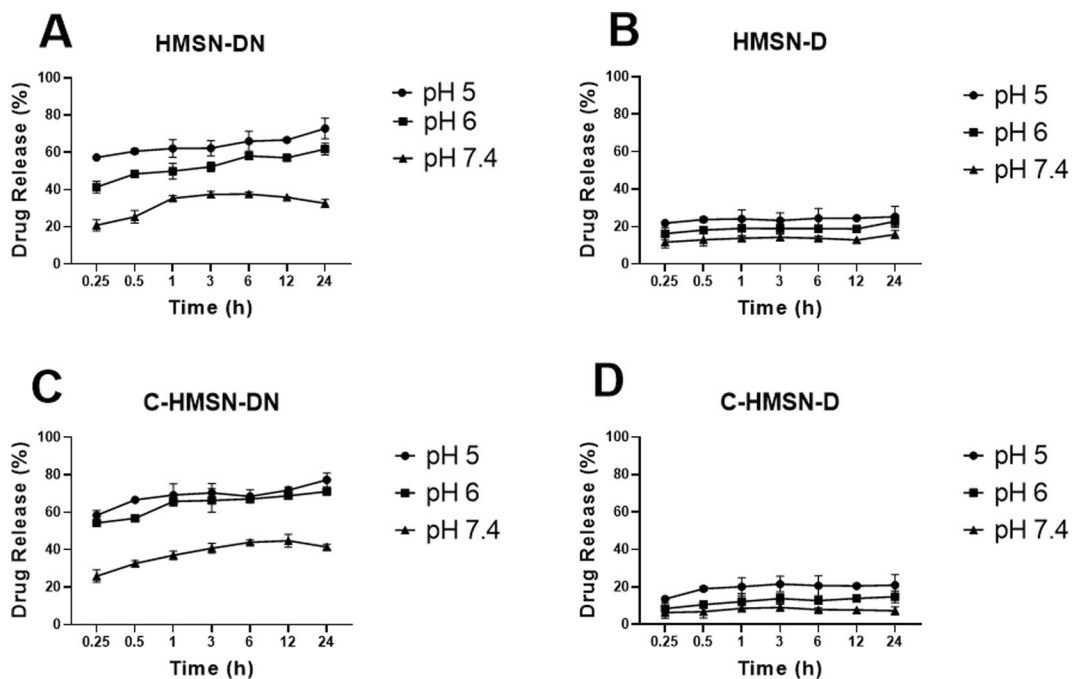


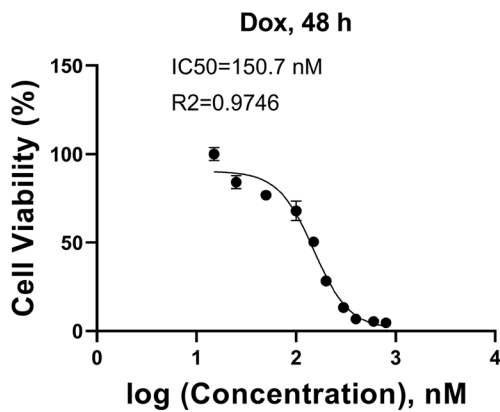
Fig. 3 Drug release results at different pHs of chitosan-coated and uncoated formulations with/without sodium bicarbonate loading. HMSN-D and HMSN-DN represent dox-loaded hollow mesoporous silica nanoparticles with and without

sodium bicarbonate co-loading, respectively. C-HMSN-D and C-HMSN-DN represent dox-loaded chitosan-PEG-coated hollow mesoporous silica nanoparticles with and without sodium bicarbonate co-loading, respectively

between HMSN-D and C-HMSN-D at any pH which is presented in Fig. 3B and C; similarly, no significant difference was observed between the formulations HMSN-CN and C-HMSN-CN which can be seen in Fig. 3A and C. These observations suggest that Cs-PEG coating does not affect the drug release, increasing pH limits the drug release, and NaHCO₃ co-loading increases the drug release.

Cell culture

Drug release results show that the NaHCO₃ loading is promising. The in vitro studies were performed for both 4 formulations to perceive the difference. Cytotoxicity of the formulations was evaluated by MTT assay using the HL60 cell line (Fig. 4). IC₅₀ of Dox was calculated as 150 nM at 48 h (Fig. 4A), and the rest of the cell culture



Concentration, nM	log (concentration)
50	1,698970004
100	2
200	2,301029996
400	2,602059991
800	2,903089987
1600	3,204119983
3200	3,505149978
6400	3,806179974
12800	4,10720997
25600	4,408239965

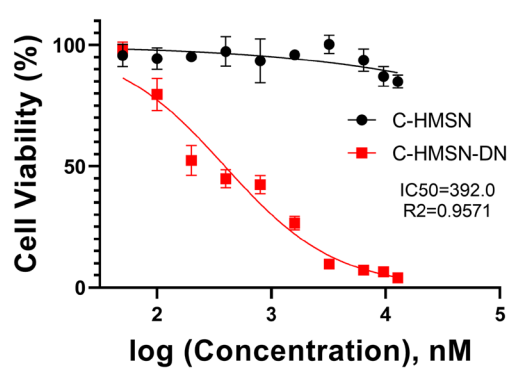
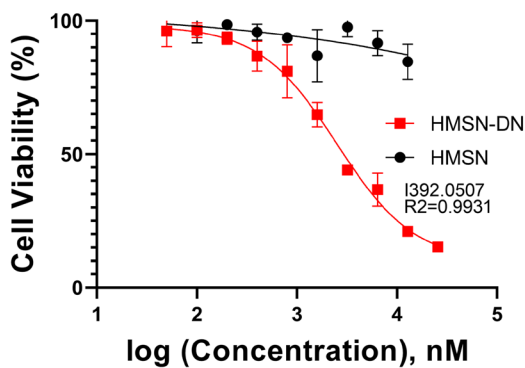
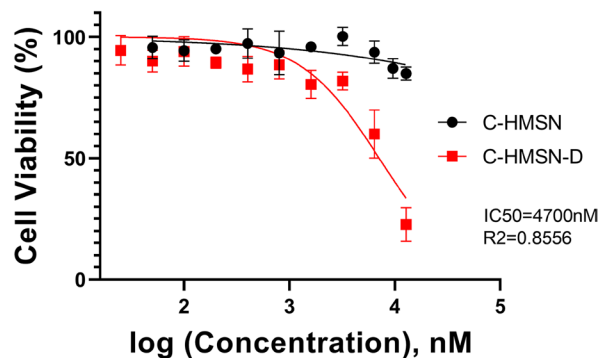
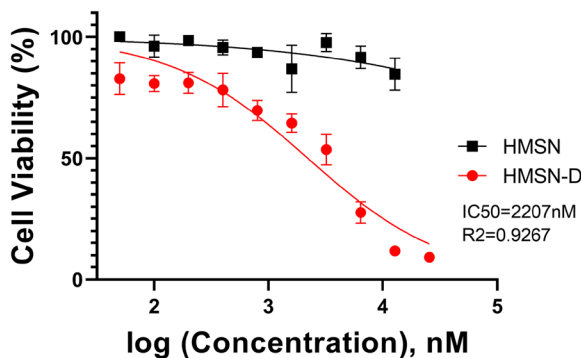


Fig. 4 Cell viability assay by MTT results. **A** IC₅₀ graph of free Dox at 48 h. **B** shows HMSN and HMSN-D and IC₅₀ value of Dox in NPs. **C** shows chitosan-coated HMSN both

Dox loaded and unloaded. **D** shows NaHCO₃ loading as HMSN and HMSN-DN and **E** shows the final formulation with and without Dox loading

studies were performed for 48 h. All the concentrations were calculated considering Dox loading efficacy, and IC₅₀s were calculated for the Dox concentrations. For each condition, blank NP formulations (formulations without Dox loading) were applied to the cells to evaluate the cytotoxicity of NPs (also applied on the L929 cell line and the results can be seen in Fig. S5). The blank NPs caused no cell death at the selected concentrations although the apoptosis was initiated by the formulations with Dox loading (Fig. 4).

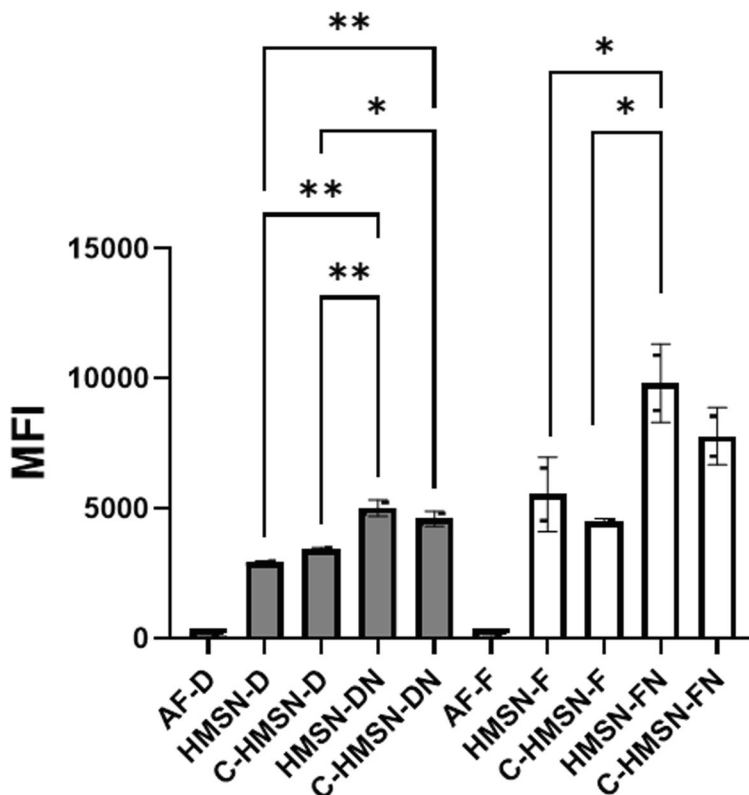
The efficiency of formulations was evaluated by performing an MTT assay in the HL60 cell line for free Dox, blank nanocarriers (HMSN and C-HMSN), and the loaded formulations (HMSN-D, HMSN-DN, C-HMSN-D, and C-HMSN-DN). The results are presented in Fig. 4. The anticancer effect of Dox was confirmed by calculation of IC₅₀ as 150 ± 7.3 nM. The concentrations between 50 and 25,600 nM were tried to determine the toxicity of blank nanocarriers which showed no obvious toxicity. Additionally, cell viabilities were decreased in the correlation of loaded formulations' concentrations. These demonstrated that the cytotoxicity is related to Dox amount released from formulations.

Moreover, IC₅₀ values of free Dox, C-HMSN-D, and C-HMSN-DN were 150 ± 7.3 nM, 2207 ± 11.5 nM, and 392 ± 6.1 nM, respectively. The decreased cytotoxicity of Dox delivered by formulations compared to the free Dox can be due to the Dox release controllability gradually increased from the free drug to HMSN which was shown in the drug release experiment. Therefore, HMSN can be regarded as biocompatible nanocarriers with the successful delivery of Dox to the cells.

From Fig. 4, it can be seen the IC₅₀ of C-HMSN-DN was lower than the other formulations as approximately 400 nM which means it is more effective as a drug carrier. While HMSNs were not cytotoxic, HMSN-D, C-HMSN-D, and HMSN-DN showed similar cytotoxicity (IC₅₀ values were calculated as 2207 nM, 4700 nM, and 2500 nM respectively). The most effective formulation was C-HMSN-DN with an IC₅₀ 392 nM which is close to free Dox. HMSNs elicit higher IC₅₀ values than Dox since the drug release takes longer.

The cellular uptake of the NPs was evaluated by a flow cytometer. HMSN-DN showed the highest uptake among the formulations according to flow cytometer results (see Fig. 5). This result supports the

Fig. 5 Cellular uptake results by flow cytometer and statistical analysis by ANOVA (error bars were given as standard deviation. * shows statistically significance, $p < 0.05$, and ** means $p < 0.005$)



idea that NaHCO_3 promotes the drug release since both formulations with NaHCO_3 were showed higher cellular uptake than the other formulations. The HMSNs were tagged with FITC via a chemical conjugation method to clarify the uptake of NPs. The formulations with NaHCO_3 showed a higher uptake (Fig. 5). It can be argued that the Dox was delivered to the cells by NPs and endosomal escape was achieved according to this data. Besides this, chitosan coating shows no effect on cellular uptake, yet the presence of NaHCO_3 increases the cellular uptake significantly as intended. The cellular uptake of HMSN-D was lower than HMSN-DN and C-HMSN-DN (statistically significant, $p < 0.005$). Similarly, C-HMSN-D showed lower cellular uptake than HMSN-DN and C-HMSN-DN (statistically significant, $p < 0.005$ and $p < 0.5$ respectively). This suggests that cellular uptake of Dox increases due to the presence of NaHCO_3 in the media. Although it is known that the presence of NaHCO_3 in the environment increases drug release, FITC was attached to the nanoparticles instead of Dox loading and given to the cells to investigate whether this release started inside or outside of the cell. The results show that the nanoparticles were uptaken by cells, and the difference between HMSN-FN and the formulations without NaHCO_3 was statistically significant ($p < 0.05$). Generally, Cs-PEG coating did not improve the cellular uptake according to Fig. 5. This probably the result of PEGylation which can lower the NP-cell interactions. Glorani et al. showed that silica nanoparticle-cell interactions reduce at PEGylated nanoparticles (Glorani et al. 2017) and our data also suggests the same.

FITC-conjugated nanoparticles are close to the nucleus according to Fig. 6. HMSN-DN and C-HMSN-DN show higher Dox in the nucleus than HMSN-D and C-HMSN-D, and this is consistent with the flow cytometer results and drug release study. NPs were close to the nucleus, and this suggests drug release was occurred after cellular uptake, according to Fig. 6. HMSN-DN and C-HMSN-DN have better interaction with the nucleus, according to Fig. 6.

Animal study

The main target of the animal study was the evaluation of the effect of Cs-PEG coating on blood circulation time. For this reason, formulations named C-HMSN-DN and HMSN-DN were administrated through the lateral tail vein of the rats, and free Dox

was applied to another group as control. The blood samples were collected after each time points (5, 30 min and 2, 8, and 24 h), and serums were separated by centrifuge. The results were presented in Fig. 7.

Free doxorubicin was not observed in any formulations according to HPLC results, while the internal standard (daunorubicin) was observed in each sample, which means that Dox was eliminated from blood almost instantly and literature supports this phenomenon (Xu et al. 2017). Besides this, Dox from the other formulations was determined in blood samples. The difference between group 2 (HMSN-DN injected) and group 3 (C-HMSN-DN injected) at each time point was statistically significant ($p < 0.0001$ at 0.083, 0.5, and 2nd h and $p < 0.05$ at 8th h) according to Fig. 7. A higher concentration of Dox was observed at the first time points of group 2. However, at the end of the 2nd h, Dox from HMSN-DN was eliminated from the blood. The blood concentration of Dox in the 5th min of C-HMSN-DN was lower than the HMSN-DN at first, yet a higher concentration was observed in the 2nd h. The experiment was terminated at the end of 24 h, and even at this time, Dox still can be observed in blood samples of group 3. The absence of a significant difference between the 8th h and the 24th h concentrations of group 3 implies that there may be a longer blood circulation time could be obtained.

Due to the wide range of usage in cancer treatment, there are numerous studies of doxorubicin as nanoparticulate drug delivery systems including silica nanoparticles (Tacar et al. 2013; Mekaru et al. 2015). Among the Dox-loaded drug delivery system, porous silica nanoparticles, especially HMSN, draw attention due to offering massive drug loading area. One of the first studies on Dox-loaded HMSN was carried out by Gao et al. (Gao et al. 2011). They reported that Dox-loaded HMSN showed a pH-responsive drug release due to their electrostatic attraction, and this system could be very promising for cancer treatment. It is known that one of the most outstanding advantages of porous silica nanoparticles is sealing the pore with stimuli-responsive gatekeepers such as lipids (Han et al. 2015), polymers (Radu et al. 2004), biomacromolecules (Zhao et al. 2014), and peptides (Sun et al. 2012). Cai and co-workers show that apart from improving the pH-dependent drug release, chitosan also increases the biocompatibility and stability of HMSNs (Cai et al. 2020). Based on these studies, chitosan-modified

Fig. 6 Cellular uptake images by fluorescence microscopy. The first row shows the nucleus, the second row shows Dox/FITC, and the third row shows the merged image

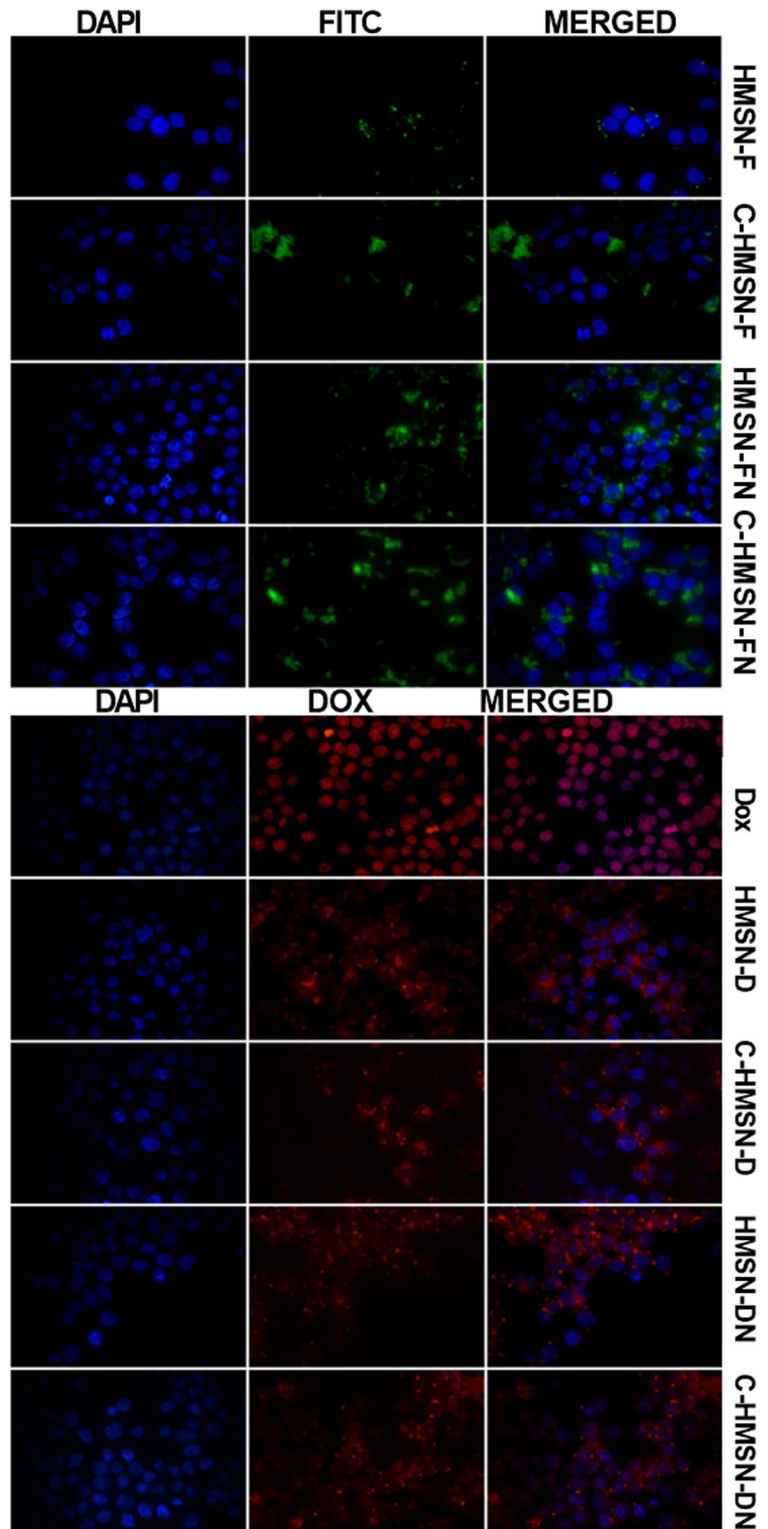
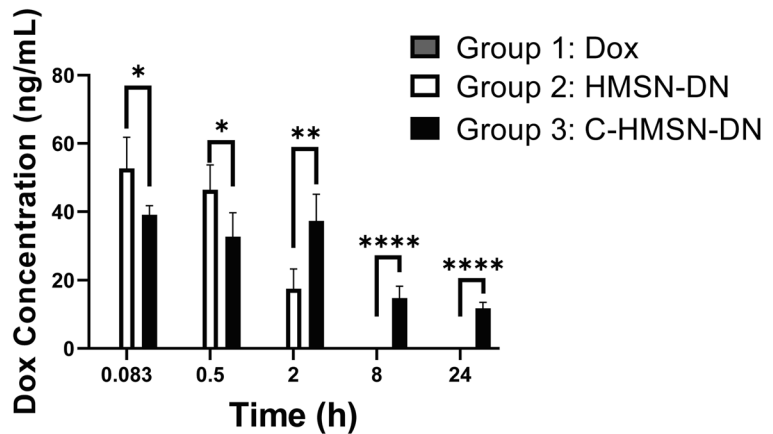


Fig. 7 Animal study results by Dox extraction from blood at different time points. Only Dox HMSN-DN and C-HMSN-DN formulations were administered to group 1, group 2, and group 3 respectively. Dox was not detected from the first time point. (*T* test was performed. **** means $p < 0.0001$), ** means $p < 0.005$, * means $p < 0.005$, and *ns* means not significant)



Dox-loaded HMSN offers decent advantages in cancer treatment but further modification could improve the effect. In our study, apart from the current advantages of chitosan, using pegylated chitosan was used to improve blood circulation time of HMSN and EPR effect. Moreover, to our knowledge, co-delivery of NaHCO_3 with Dox in HMSN has been performed the first time. In a recent study, NaHCO_3 was used as an adjuvant in doxorubicin-loaded liposome formulation, and the efficiency of the system was researched in 4T1 breast cancer cells (Abumanhal-Masarweh et al. 2019). It is found that obtained system improves the therapeutic outcome compared to mice treated with Dox and NaHCO_3 alone. Our study also confirmed these results.

Conclusion

Although the survival rate has increased in recent years, AML can still be fatal to many patients, and new approaches are needed for improving patient compliance. Doxorubicin is one of the most effective cancer drugs, yet the clinic use is relatively limited due to the dose limitations caused by the fast elimination from the blood. To overcome these limitations and provide a prolonged blood circulation time, PEGylation is one of the best alternatives. In this study, we present a drug delivery system that provides a prolonged blood circulation time due to Cs-PEG coating and effective drug delivery via pH-sensitive drug release and endosomal escape for AML treatment. NaHCO_3 co-loading improved the DDS efficiency (IC₅₀ was smaller than the formulations without NaHCO_3) which suggests

that the endosomal escape is achieved. Cs-PEG prolonged the blood circulation time and even after 24 h Dox was still observed in the blood. Myeloid cells are granular cells containing a great number of lysosomes. Considering this, the designed DDS can be more effective by endosomal escape to eliminate these cells from the blood.

Acknowledgements TEM, SEM, XRD, and BET analyses were performed in Middle East Technical University Central Laboratory. Special thanks to ILKO ARGEM for FTIR analysis. A part of this study was supported by Hacettepe University Coordinatorship of Scientific Research Projects with the project code THD-2016-12890. Special thanks to Prof. Fernandez-Megia and his team for giving Chitosan-PEG as a kind gift. Also, thanks to DEVA Holding A.S. for doxorubicin which was a kind gift from them.

Declarations

Conflict of interest The authors declare that they have no conflict of interest.

References

- Abumanhal-Masarweh H, Koren L, Zinger A, Yaari Z, Krinsky N, Kaneti G, Dahan N, Lupu-Haber Y, Suss-Toby E, Weiss-Messer E, Schlesinger-Laufer M, Shainsky-Roitman J, Schroeder A (2019) Sodium bicarbonate nanoparticles modulate the tumor pH and enhance the cellular uptake of doxorubicin. *J Control Release* 296:1–13
- Bagwe RP, Hilliard LR, Tan W (2006) Surface modification of silica nanoparticles to reduce aggregation and nonspecific binding. *Langmuir* 22:4357–4362
- Behzadi S, Serpooshan V, Tao W, Hamaly MA, Alkawareek MY, Dreaden EC, Brown D, Alkilany AM, Farokhzad OC, Mahmoudi M (2017) Cellular uptake of nanoparticles: journey inside the cell. *Chem Soc Rev* 46:4218–4244

- Cai D, Han C, Liu C, Ma X, Qian J, Zhou J, Li Y, Sun Y, Zhang C, Zhu W (2020) Chitosan-capped enzyme-responsive hollow mesoporous silica nanoplatforms for colon-specific drug delivery. *Nanoscale Res Lett* 15:123
- Chen Y, Chen H, Guo L, He Q, Chen F, Zhou J, Feng J, Shi J (2010) Hollow/rattle-type mesoporous nanostructures by a structural difference-based selective etching strategy. *ACS Nano* 4:529–539
- Chen Y, Yang W, Chang B, Hu H, Fang X, Sha X (2013) In vivo distribution and antitumor activity of doxorubicin-loaded N-isopropylacrylamide-co-methacrylic acid coated mesoporous silica nanoparticles and safety evaluation. *Eur J Pharm Biopharm* 85:406–412
- Daeihamed M, Haeri A, Dadashzadeh S (2015) A simple and sensitive HPLC method for fluorescence quantitation of doxorubicin in micro-volume plasma: applications to pharmacokinetic studies in rats, Iran. *J Pharm Res* 14:33–42
- Daryasari MP, Akhgar MR, Mamashli F, Bigdeli B, Khoobi M (2016) Chitosan-folate coated mesoporous silica nanoparticles as a smart and pH-sensitive system for curcumin delivery. *RSC Adv* 6:105578–105588
- Fang X, Chen C, Liu Z, Liu P, Zheng N (2011) A cationic surfactant assisted selective etching strategy to hollow mesoporous silica spheres. *Nanoscale* 3:1632–1639
- Fang X, Zhao X, Fang W, Chen C, Zheng N (2013) Self-templating synthesis of hollow mesoporous silica and their applications in catalysis and drug delivery. *Nanoscale* 5:2205–2218
- Feng W, Nie W, He C, Zhou X, Chen L, Qiu K, Wang W, Yin Z (2014) Effect of pH-responsive alginate/chitosan multilayers coating on delivery efficiency, cellular uptake and biodistribution of mesoporous silica nanoparticles based nanocarriers. *ACS Appl Mater Interfaces* 6:8447–8460
- Fleischer CC, Payne CK (2014) Nanoparticle-cell interactions: molecular structure of the protein corona and cellular outcomes. *Acc Chem Res* 47:2651–2659
- Gao Y, Chen Y, Ji X, He X, Yin Q, Zhang Z, Shi J, Li Y (2011) Controlled intracellular release of doxorubicin in multidrug-resistant cancer cells by tuning the shell-pore sizes of mesoporous silica nanoparticles. *ACS Nano* 5:9788–9798
- García-Fernández A, Aznar E, Martínez-Mañez R, Sancenón F (2020) New advances in in vivo applications of gated mesoporous silica as drug delivery nanocarriers. *Small* 16:1902242
- Glorani G, Marin R, Canton P, Pinto M, Conti G, Fracasso G, Riello P (2017) Pegylated silica nanoparticles: cytotoxicity and macrophage uptake. *J Nanopart Res* 19:294
- Gunawan C, Lim M, Marquis CP, Amal R (2014) Nanoparticle-protein corona complexes govern the biological fates and functions of nanoparticles. *J Mater Chem B* 2:2060–2083
- Han N, Zhao Q, Wan L, Wang Y, Gao Y, Wang P, Wang Z, Zhang J, Jiang T, Wang S (2015) Hybrid lipid-capped mesoporous silica for stimuli-responsive drug release and overcoming multidrug resistance. *ACS Appl Mater Interfaces* 7:3342–3351
- Herd H, Daum N, Jones AT, Huwer H, Ghandehari H, Lehr CM (2013) Nanoparticle geometry and surface orientation influence mode of cellular uptake. *ACS Nano* 7:1961–1973
- Inocêncio S, Cordeiro T, Matos I, Danêde F, Sotomayor JC, Fonseca IM, Correia NT, Corvo MC, Dionísio M (2021) Ibuprofen incorporated into unmodified and modified mesoporous silica: from matrix synthesis to drug release. *Microporous Mesoporous Mater* 310:110541
- Kaasalainen M, Aseyev V, von Haartman E, Karaman DŞ, Mäkilä E, Tenhu H, Rosenholm J, Salonen J (2017) Size, stability, and porosity of mesoporous nanoparticles characterized with light scattering. *Nanoscale Res Lett* 12:74
- Kanwal U, Irfan Bukhari N, Ovais M, Abass N, Hussain K, Raza A (2018) Advances in nano-delivery systems for doxorubicin: an updated insight. *J Drug Target* 26:296–310
- Ke C-J, Su T-Y, Chen H-L, Liu H-L, Chiang W-L, Chu P-C, Xia Y, Sung H-W (2011) Smart multifunctional hollow microspheres for the quick release of drugs in intracellular lysosomal compartments. *Angew Chem Int Ed* 50:8086–8089
- Krischke M, Hempel G, Völler S, André N, D’Incalci M, Bisogno G, Köpcke W, Borowski M, Herold R, Boddy AV, Boos J (2016) Pharmacokinetic and pharmacodynamic study of doxorubicin in children with cancer: results of a “European Pediatric Oncology Off-patents Medicines Consortium” trial. *Cancer Chemother Pharmacol* 78:1175–1184
- Llopis-Lorente A, Lozano-Torres B, Bernardos A, Martínez-Mañez R, Sancenón F (2017) Mesoporous silica materials for controlled delivery based on enzymes. *J Mater Chem B* 5:3069–3083
- Mekaru H, Lu J, Tamanoi F (2015) Development of mesoporous silica-based nanoparticles with controlled release capability for cancer therapy. *Adv Drug Deliv Rev* 95:40–49
- Pisani C, Gaillard JC, Odorico M, Nyalosaso JL, Charnay C, Guari Y, Chopineau J, Devoisselle JM, Armengaud J, Prat O (2017) The timeline of corona formation around silica nanocarriers highlights the role of the protein interactome. *Nanoscale* 9:1840–1851
- Popat A, Liu J, Lu GQ, Qiao SZ (2012) A pH-responsive drug delivery system based on chitosan coated mesoporous silica nanoparticles. *J Mater Chem* 22:11173–11178
- Radu DR, Lai C-Y, Jeftinija K, Rowe EW, Jeftinija S, Lin VSY (2004) A polyamidoamine dendrimer-capped mesoporous silica nanosphere-based gene transfection reagent. *J Am Chem Soc* 126:13216–13217
- Rawal M (2018) CHAPTER 2 Materials and chemistry of stimuli-responsive drug delivery systems, stimuli-responsive drug delivery systems. *R Soc Chem* 33–50
- Robbins SL, Kumar V (2008) Robbins temel patoloji: (basic pathology), Nobel Tip Kitabevi
- Roca M, Haes AJ (2008) Silica–void–gold nanoparticles: temporally stable surface-enhanced Raman scattering substrates. *J Am Chem Soc* 130:14273–14279
- Stewart BW, Wild C (2014) World cancer report 2014. International Agency for Research on Cancer, WHO Press, Lyon
- Suk JS, Xu Q, Kim N, Hanes J, Ensign LM (2016) PEGylation as a strategy for improving nanoparticle-based drug and gene delivery. *Adv Drug Deliv Rev* 99:28–51

- Sun Y-L, Yang B-J, Zhang SX-A, Yang Y-W (2012) Cucurbit [7] uril pseudorotaxane-based photoresponsive supramolecular nanovalve. *Chem Eur J* 18:9212–9216
- Szegedi A, Popova M, Goshev I, Klébert S, Mihály J (2012) Controlled drug release on amine functionalized spherical MCM-41. *J Solid State Chem* 194:257–263
- Tacar O, Sriamornsak P, Dass CR (2013) Doxorubicin: an update on anticancer molecular action, toxicity and novel drug delivery systems. *J Pharm Pharmacol* 65:157–170
- Teng Z, Su X, Zheng Y, Sun J, Chen G, Tian C, Wang J, Li H, Zhao Y, Lu G (2013) Mesoporous silica hollow spheres with ordered radial mesochannels by a spontaneous self-transformation approach. *Chem Mater* 98–105
- Torchilin VP (2018) CHAPTER 1 Fundamentals of stimuli-responsive drug and gene delivery systems, stimuli-responsive drug delivery systems. *R Soc Chem* 1–32
- Tuoriniemi J, Johnsson A-CJH, Holmberg JP, Gustafsson S, Gallego-Urrea JA, Olsson E, Pettersson JBC, Hassellöv M (2014) Intermethod comparison of the particle size distributions of colloidal silica nanoparticles. *Sci Technol Adv Mater* 15:035009
- Varkouhi AK, Scholte M, Storm G, Haisma HJ (2011) Endosomal escape pathways for delivery of biologicals. *J Control Release* 151:220–228
- Wang Z, Zhang X, Huang G, Gao J (2018) CHAPTER 3 pH-responsive drug delivery systems, stimuli-responsive drug delivery systems. *R Soc Chem* 51–82
- Xiong L, Du X, Kleitz F, Qiao SZ (2015) Cancer-cell-specific nuclear-targeted drug delivery by dual-ligand-modified mesoporous silica nanoparticles. *Small* 11:5919–5926
- Xu P, Zuo H, Chen B, Wang R, Ahmed A, Hu Y, Ouyang J (2017) Doxorubicin-loaded platelets as a smart drug delivery system: an improved therapy for lymphoma. *Sci Rep* 7:42632
- Yoo S, Lee J, Kim JM, Seong CY, Seong KD, Piao Y (2016) Well-dispersed sulfur wrapped in reduced graphene oxide nanoscroll as cathode material for lithium-sulfur battery. *J Electroanal Chem* 780:19–25
- Zhao Q, Wang C, Liu Y, Wang J, Gao Y, Zhang X, Jiang T, Wang S (2014) PEGylated mesoporous silica as a redox-responsive drug delivery system for loading thiol-containing drugs. *Int J Pharm* 477:613–622
- Zhu Y, Fang Y, Borchardt L, Kaskel S (2011) PEGylated hollow mesoporous silica nanoparticles as potential drug delivery vehicles. *Microporous Mesoporous Mater* 141:199–206

Publisher's Note Springer Nature remains neutral with regard to jurisdictional claims in published maps and institutional affiliations.